

Effect of Trapped Charges on Cable SVL Failure

F Ghassemi

Abstract-- Excessive sheath voltage limiters (SVL) failures were observed in at least three of the 275 kV circuits in National Grid network, which in turn led to extra cost, more frequent and longer maintenance interventions.

The ATP-EMTP programme is used to model a cable circuit with high SVL failure rate. This paper presents results of the investigation. It will be shown that although the SVLs should withstand the surges for normal switching and external fault conditions, but their energy absorption rating is exceeded if the cable is energised while it has high level of trapped charges with opposite polarity to switching voltages. The operational switching log confirmed that the cables with high SVL failures are those which were used as a means of voltage control during light load conditions and that when they are switched daily for this purpose there is no discharge path for the charge drainage. Short and long term remedies are proposed to resolve the issues.

Keyword : ATP-EMTP, cable sheath transients, SVL failure.

I. BACKGROUND

THE use of single-phase power cables in Extra High Voltage (EHV) transmission systems may necessitate the application of sheath interruption and special bonding arrangements of the sheath to eliminate or reduce the induced sheath currents which otherwise would limit the loading capacity of the cable system. In cables longer than about 1 km crossbonding of the sheath has been generally adopted. Different types of crossbonding can be used. Each short section, known as minor crossbonding junction, is connected to ground via sheath voltage limiter (SVL). These are usually made of metal oxide varistor (MOV) which have very high nonlinear characteristic. Every several minor section the sheath of three phases are bonded together and connected to ground. The cable section between two grounded points is called a major section which would consist of several minor sections. Full reduction of sheath currents is achieved if the sheath or core circuits have a cyclic transposition of roughly equal length.

A disadvantage of sheath interruption is that the normal coaxial arrangement of conductor and/or sheath within the cable is disturbed [1]. Incoming surges due to lightning, switching operations and faults will be submitted to partial reflection and refraction when they pass a sheath joint. This gives rise to overvoltages across the sheath section insulation and across the sheath to earth insulation [1] – [4].

Foroozan Ghassemi is with National Grid Electricity Transmission National Grid House, Warwick Technology Park, Gallows Hill, Warwick EC34 6DA, United Kingdom.

Email: forooz.ghassemi@nationalgrid.com

Paper submitted to the International Conference on Power Systems Transients (IPST2013) in Vancouver, Canada, July 18-20, 2013.

National Grid, the Great Britain (GB) grid operator, own a large asset of cable circuits at 275 and 400 kV level. Excessive sheath voltage limiters (SVL) failures were detected in at least three of the 275 kV circuits during routine maintenance. This in turn led to extra cost, more frequent and longer maintenance interventions. It is also noted, from the operational log, that the cables with high SVL failure are those that are switched during night in light load condition to control the voltage magnitude in the area.

A study was carried out to investigate the root cause of excessive SVL failures. ATP-EMTP programme was used to model a cable circuit with high SVL failure rate.

II. NETWORK DESCRIPTION

The cable circuit considered in the study consists of two parallel, three-phase, 275 kV cables. Each circuit consists of three single phase cables. They connect Substations (S/S) A and B. The cable detail is given in Appendix A. Fig. 1 illustrates the crossbonding used in the cable installation considered in the study. The cores are transposed at every junction, which leads to more balanced impedances in all three phases. The sheaths are crossbonded as shown in junction box illustration on the left hand side of Fig. 1. By crossbonding the cable sheaths the induced current in the sheath during load condition is reduced.

For security of supply and reliability purposes, the circuits are on average about 5 m apart and they are placed in different trenches with an average depth of 1 m. Two crossbonding points with SVLs exist within each major section, which in turn corresponds to three cable minor sections. As shown in Fig. 1 the sheaths are solidly connected to earth at major section points which is illustrated by the junction box representation on the right hand side of Fig. 1. Table I shows the length of minor and major sections in meters (m) with corresponding junction box (JB) numbers. The longest minor section length is 1651.71 m for Circuit 1 (CCT1) and 1806.85 m for Circuit 2 (CCT2). The longest major sections are 4610.71 m and 5079.19 m respectively for CCT1 and CCT2. The shortest major sections are 3035.20 m and 3012.03 m for CCT1 and CCT2 from S/S B. The total length of CCT1 and CCT2 are respectively 21.25 km and 21.74 km.

Layout for Substation (S/S) A and B are shown in Fig. 2 and Fig. 3 respectively. DNO and TO stand for distribution network operator and transmission operator respectively. Only part of the equipment related and significant to the study is shown. Isolator switch L21 and L22 in S/S A and B are isolators with load-break and fault-make capability only. These are used to switch CCT2 in or out without operating the main busbar circuit breaker. Note that the busbar and main circuit breakers format is such that by isolating a busbar mesh corner, transformers supplying the distribution network are also interrupted and therefore cannot be used regularly to disconnect the cables.

For operational reasons, L22 in S/S B is used to charge the cable and then L21 is closed in S/S A. There is no isolator switch on CCT1 and therefore it cannot be switched without operating the main busbar circuit breakers.

Note that the instrument transformer connected to the cables are of capacitive voltage transformer (CVT) type with no dc coupling, which means that it has very high impedance at dc.

TABLE I
MINOR SECTIONS LENGTH

| Cross-bonding Type | Circuit 1 | | | Circuit 2 | | |
|--------------------|------------------|------------------|--------------|------------------|------------------|--------------|
| | Minor Length (m) | Major Length (m) | JB | Minor Length (m) | Major Length (m) | JB |
| Earthing | 0.00 | | | S/S A | 0.00 | |
| Minor | 1357.28 | 4487.27 | | S/S A | | |
| Minor | 1478.28 | | 1-174 | 1547.77 | | 2-174 |
| Major | 1651.71 | | 1-167 | 1724.56 | | 2-167 |
| Major | 1651.71 | | 1-160 | 1806.85 | | 2-160 |
| Minor | 1511.20 | 4525.97 | 1-154 | 1441.40 | | 2-154 |
| Minor | 1528.27 | | 1-148 | 1522.17 | 4481.47 | 2-148 |
| Major | 1486.51 | | 1-142 | 1517.90 | | 2-142 |
| Minor | 1534.36 | 4596.69 | 1-136 | 1488.64 | | 2-136 |
| Minor | 1509.06 | | 1-130 | 1545.34 | 4561.94 | 2-130 |
| Major | 1553.26 | | 1-124 | 1527.96 | | 2-124 |
| Minor | 1512.11 | 4610.71 | 1-118 | 1530.71 | | 2-118 |
| Minor | 1534.36 | | 1-112 | 1534.67 | | 2-112 |
| Major | 1564.23 | | 1-106 | 1537.72 | | 2-106 |
| Minor | 1032.97 | 3035.20 | 1-102 | 1037.23 | | 2-102 |
| Minor | 1024.43 | | 1-098 | 988.77 | 3012.03 | 2-098 |
| Earthing | 977.80 | | | S/S B | 986.03 | |

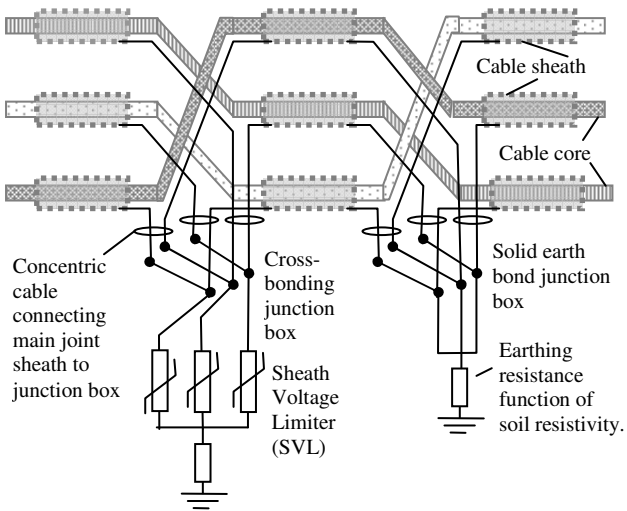


Fig. 1. Cable Crossbonding Method.

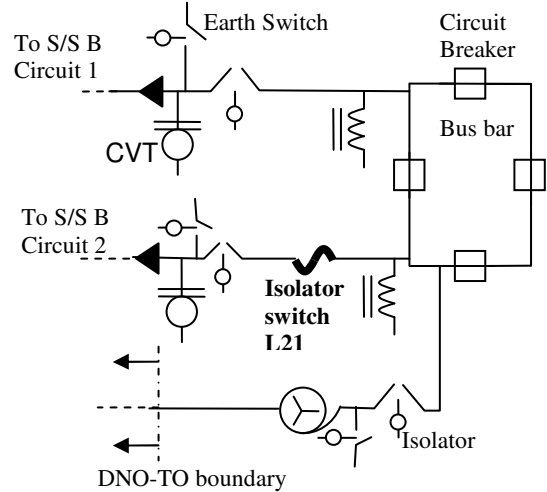


Fig. 2. Substation A Layout-Study Related Components.

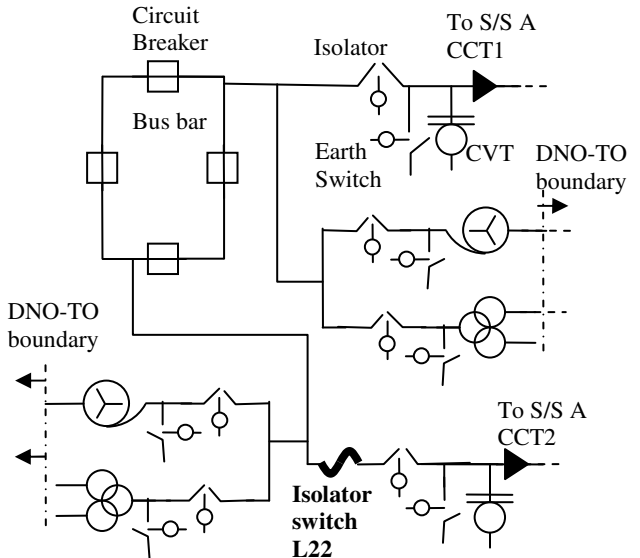


Fig. 3. Substation B Layout-Study related Components.

III. NETWORK MODEL

ATP-EMTP programme is used to model the network. The double circuit cables between S/S A and B together with surrounding substations, cable and overhead line circuits are modelled. The main cable circuits under investigation are modelled in detail which includes detailed solid and cross bonding junction boxes including coaxial cables.

The starting point to set up the model is to decide about the boundary points within which the network is modelled with as much detail as possible and when the rest of the network is reduced and represented as equivalent sources. This is necessary to optimise the simulation speed and time to set up the model. As per recommendation in [5] at least two substations away from the points of interest (S/S A and B) are considered. The other consideration is to select boundary points with minimum short circuit current coupling between them such that fault current in one boundary point does not include large contribution from other sources (boundary points) in the model. These requirements led to a network with four boundary points, B1 to B4 and three internal nodes, as

shown in Fig. 4. The network data is given in Appendix B.

Node B1 is the next substation from S/S A but because it is a 400 kV substation and there are two 900 MVA transformers between the two substations they are not considered to be electrically close and therefore it is assumed that the switching overvoltages are not affected by the inaccuracies in the source impedance representation at Node B1.

There are different methods to reduce a network to its Thevenin equivalent that is also valid for wide bandwidth study such as switching analysis [5], [6]. In this study the sources at the boundary points are modelled as distributed parameter transmission line. Series R and X parameters are those obtained from short circuit analysis and the capacitance at the node is the sum of the capacitance of all lines/cables connected to the busbar. All series and capacitance parameters are calculated while the elements and equipment, e.g. lines, cables, shunt capacitor and reactors, which are included in the detailed model, are disconnected. As the boundary nodes are electrically far from the study points of interest the source equivalent representation is deemed adequate as the variation in source impedance and susceptance at the boundary points did not greatly affect overvoltages in S/S A and B. Furthermore, in order to control short circuit current the normal running arrangements for Node B1 and Node B3 are split busbar. Therefore, the short circuit current mutual coupling between the busbars in the substation should be represented. Also, it is found that fault current coupling between Node B3 and Node B4 exists. All mutual coupling between boundary nodes are represented by lumped line positive and zero sequence model.

There is a quad booster (phase shifter transformer) in Node B4. This is represented by a series lumped resistance/reactance model.

All cables, except the cables between S/S A and B are modelled as distributed parameter.

The lines are modelled as LCC elements with their tower and conductor geometry included. Equivalent Π model is used for system frequency (50 Hz) short circuit analysis. For switching analysis JMarti model is used where the frequency for calculating transformation matrix is set at 500 Hz in accordance with the recommendations in [7].

The loads are represented at the LV side of supergrid autotransformers at 132 kV and some at 66 kV. The load model has been developed by the GB power industry for wide bandwidth studies. For fault inception and clearance, temporary overvoltage and general switching studies, it is essential to include as much detail as possible for transformers supplying loads and the load itself. However, it is found that the conclusion of the study for sheath overvoltages is not greatly affected by the load and transformer models and therefore data for these elements is not given in this paper. It is however observed that in steady state load conditions high level of triplen harmonics, generated by the core non-linearity flow in the cable sheath.

Transformers are modelled as BCTRAN with magnetising branch together with non-linear core losses included. Data for transformers are obtained from factory test sheets, which provide no-load data up to 110% of nominal voltage. In accordance with the recommendation in [6] a magnetising reactance corresponding to four times the air core reactance is

considered for applied voltage of 120%. Terminal capacitance is considered in accordance with [5]

In S/S A and B, all transformers star points, cable sheaths and other substation equipment are connected to earth mat impedance (at 50 Hz) of $0.11\angle 20^\circ \Omega$ and $0.1\angle 10^\circ \Omega$ respectively, which are obtained from earthing measurement database.

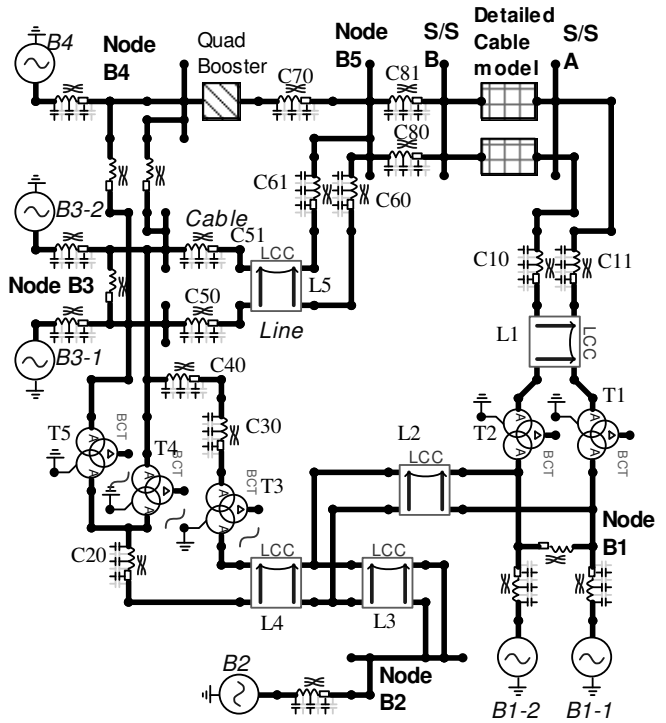


Fig. 4. Network Schematic Considered.

IV. CABLES DETAILED MODEL

Each cable section is simulated as Π model for 50 Hz short circuit analysis and Bergeron model for switching studies. In order to represent the losses adequately, for switching studies the frequency at which the cable parameters are calculated is set at 5 kHz. This frequency is selected due to the sheath short sections created by crossbonding and earthing junctions.

The SVL used in the original design were SVL45, which had a voltage rating of 45 kV with energy absorption capability of 16 kJ. After high level of SVL failure was detected the SVLs were upgraded to SVL90 with 90 kV and 31 kJ voltage and energy rating respectively. The upgrade did not prevent the SVLs from failing. According to the manufacturer, SVL90 consists of two SVL45 in series in the same enclosure capsule. The SVL V-I characteristic is given in TABLE 2. Type NLINRES in ATPDraw is used to model the SVL. Several benchmarking of the V-I characteristic is carried out for 8/20 μ s impulse wave for different impulse current magnitude and the results are compared with the type test data provided by the manufacturer. Fig. 5 shows the result for 5 kA impulse where the voltage across the SVL is limited to 20 kV.

TABLE II
SVL90 V-I CHARACTERISTIC

| I (A) | V (V) |
|----------|---------|
| 0.0141 | 4242.6 |
| 0.0424 | 12727.9 |
| 0.0707 | 14142.1 |
| 0.7071 | 14849.2 |
| 1.4142 | 15556.3 |
| 2.8284 | 16263.5 |
| 6.6468 | 16617 |
| 2050.61 | 18384.8 |
| 4949.75 | 19799 |
| 10182.34 | 21213.2 |
| 15556.4 | 22344.6 |
| 43840.6 | 25455.8 |

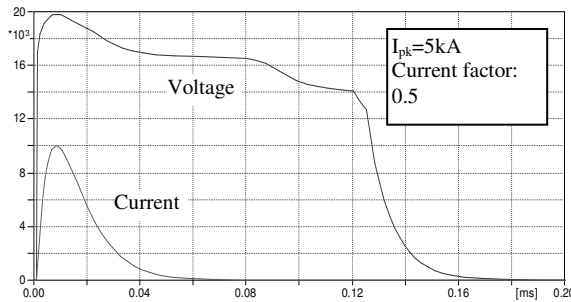


Fig. 5. SVL90 Characteristic for 5 kA, 8/20 Impulse.

In order to avoid numerical instability at the point of transition from low to high conduction regions, which in turn may lead to unrealistic high voltages, the sampling interval of the simulation is set at 50 ns but the results are saved in the output file every 0.25 μ s.

The model for crossbonding junction box is shown in Fig. 6.

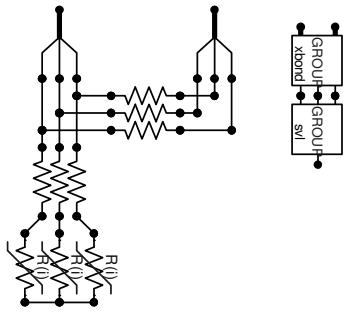


Fig. 6. Crossbonding JB Circuit and its Compact Equivalent.

The diagram on the left shows the actual circuit. The compress facility in ATPDraw is used to create an object with equivalent function to facilitate speedy set up of the model and better use of the drawing space. The use of low value (0.001Ω) linear resistors in the crossbonding circuit is necessary to avoid erroneous result which occurs when the splitters are directly connected. The voltage across and current through each SVL at all junction boxes are recorded by the simulation. At solid earth junctions the sheaths are connected to earth. A linear resistance of 15Ω is considered for the earth

connection in all junction boxes, both for solid earth and crossbonding points. According to earth resistance records this can vary from 5 to 20Ω .

For switching studies, sheath of each phase at both ends is connected to the corresponding earth mat impedance through a 0.2Ω linear resistor to represent the cable sealing end resistance at high frequencies.

Voltage and Current probes are used at all junction boxes to record sheath voltages and currents. Currents entering the substation earth mat from the cable sheaths are also recorded.

V. SYSTEM FREQUENCY ANALYSIS

The maximum load current through one circuit is approximately 1.7 kA if the other circuit is out of service (OOS). Sheath voltages for this operating condition are shown in Fig. 7. The sheath voltage is nearly zero at the solid earth junction and the maximum is 300 V. This voltage is well below the SVL conduction voltage and therefore the current through the SVL is nearly zero. The maximum sheath current is about 85A.

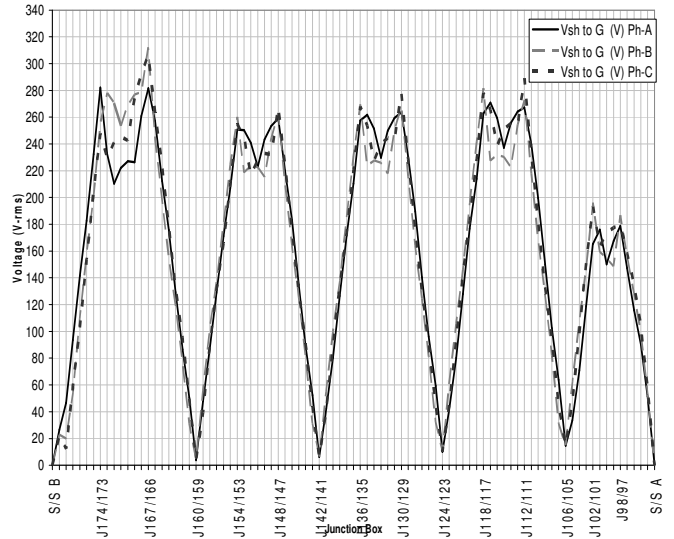


Fig. 7. CCT2 Sheath Voltage for Load Condition.

Although the main focus of the study is SVLs failure due to regular switching but cable internal and busbar single phase to ground and busbar three phase short circuit faults are considered to examine the maximum sheath voltage and hence SVLs currents during fault. For internal single phase faults, it is assumed that the short circuit occurs between the core and sheath, which leads to the sheath carrying the fault current for some distance until the first solid earth point or SVL junction is reached. According to the protection policy, the fault at 275 kV should be cleared within 120 ms. For load and cable external fault, steady state currents, the sheath voltage remains well below the SVL conduction voltage and hence no stress is imposed on the SVL. For internal core to sheath fault and depending on the fault location, the SVL rating may be exceeded and hence damage may occur if the fault clearing time is 120 ms.

VI. SWITCHING ANALYSIS

Switching and fault conditions are considered. The sheath and SVLs voltages and currents are studied for 2.5 ms after

the switching and fault inception. Significant amount of switching disturbances on the sheath disappear before 2.5 ms lapses. The study is run at 20 MHz but the results are stored at 4 MHz to optimise the storage requirement without losing accuracy. In this paper the results of transients associated with faults are not presented and the focus will be on switching transient. This is due to the fact that the cables have suffered no faults during the past few years and all SVL failures are considered to have been due to regular and daily switching activities or reasons other than circuit faults. Both synchronous and asynchronous pole closing are considered. The study examines energy absorbed by the SVL which is a function of magnitude of the voltage across and current through SVLs as well as the duration for which high current flows. TACS modules and Fortran Statement-Math Function together with compress facility in ATPDraw is used to build a probe for every SVL to output the maximum energy absorbed.

Although the switching is often carried out from S/S B but in the study switching from both substations are considered to check variation in surge severity.

As shown in Fig. 2, there are two reactors at S/S A, each of 100 MVar, connected to the same mesh corners as the cables. If these reactors are switched out together with the cables then they provide discharge path for the trapped charges on the cables. However CCT2 is switched daily by means of switch disconnectors, L21 and L22 at the two ends. Therefore there is no discharge path for the trapped charges to drain once the cable is switched out. The only path for drainage is through the insulation losses that are very low. The time the cable remains out of service is usually between late evenings to early morning of the next day. Also, during this period the reactors are needed to keep the voltage magnitude below the statutory requirement.

Preliminary simulation runs are carried out to determine the voltage on three phases of the circuit being switched when the current ceases at near zero crossing. This current is highly capacitive as it is assumed that the trapped charges are determined by the last switch to open, i.e. line dropping. In the circuit breaker model, the maximum current at which the phase current ceases is set at 50 A. This is the Imax parameter in the SWIT_3XT object of the ATPDraw. Three single phase dc sources are then used to charge the cables and then removed before the main switch is closed. This is found to be more efficient from simulation run time point of view than first opening the circuit breaker and then reclosing it which requires much longer simulation time.

About 200 study cases are considered which include different network configuration including other lines and cables outages.

TABLE III gives an abstract of the runs with and without trapped charges. The SVL energy absorption did not exceed the rating for all study cases with no trapped charges. It can be seen that if the cable is energised without any trapped charges the maximum energy absorbed by SVLs is 5.4 kJ which is associated with Run 4 and 6 and well below the rating of 31 kJ. The SVLs closer to the junction boxes from either ends are most affected by the switching from the corresponding end. The magnitude of surges reduces significantly by the time they arrive at the end of the cable. With trapped charges on the cable the energy absorbed by SVL increases significantly and

exceeds the SVL rating, if the voltage due to trapped charges has opposite polarity to the switching surges. This is likely to be the cause of the SVL failure and is particularly evident in Study case 10, 12 and 14 presented in Table IV. 100% trapped charge refers to the approximate voltage on cable prior to switching of $0.97 \times \frac{275}{\sqrt{3}} \times \sqrt{2}$ kV. Study is also carried out

with 50% trapped charge while all other parameters remain the same. The absorbed energy level would approximately reduce in proportion.

Note that Junction Box 167 is the second from S/S B. The first Junction Box, JB 174, has a lower absorption rate. The voltage appearing at SVLs terminals is a function of interactions between different surges, and their frequency content, arriving at the SVL junction. Initial switching surges would amalgamate with waves reflected from other lines and cables connected to the busbar and also depend on the busbar terminal equipment as well as the reflection from the far terminals. The SVL energy absorption is a function of the voltage magnitude and duration for which it remains in conduction state. Forensic examination has shown that when SVLs fail they are very likely to become open circuit, which in turn means that the surges produced by subsequent switching would be imposed on the next sets of the SVLs leading to chain failure.

TABLE III
STUDY CASES

KEY: S= SWITCHED, OOS= OUT OF SERVICE, IN= IN SERVICE, O= OPEN

| ID | CCT2 | CCT1 | S/S B | S/S A | Switch Time (ms) | | | COMMENT |
|----|------|------|-------|-------|------------------|------|------|-------------|
| | | | | | Ph-A | Ph-B | Ph-C | |
| 0 | S | OOS | O | S | 0.1 | 0.1 | 0.1 | No charge |
| 1 | S | OOS | O | S | 0.2 | 0.1 | 0.3 | No charge |
| 2 | S | OOS | S | O | 0.1 | 0.1 | 0.1 | No charge |
| 3 | S | OOS | S | O | 0.2 | 0.1 | 0.3 | No charge |
| 4 | S | IN | O | S | 0.1 | 0.1 | 0.1 | No charge |
| 5 | S | IN | O | S | 0.2 | 0.1 | 0.3 | No charge |
| 6 | S | IN | S | O | 0.1 | 0.1 | 0.1 | No charge |
| 7 | S | IN | S | O | 0.2 | 0.1 | 0.3 | No charge |
| 8 | S | OOS | O | S | 0.1 | 0.1 | 0.1 | 100% charge |
| 9 | S | OOS | O | S | 0.2 | 0.1 | 0.3 | 100% charge |
| 10 | S | OOS | S | O | 0.1 | 0.1 | 0.1 | 100% charge |
| 11 | S | OOS | S | O | 0.2 | 0.1 | 0.3 | 100% charge |
| 12 | S | IN | O | S | 0.1 | 0.1 | 0.1 | 100% charge |
| 13 | S | IN | O | S | 0.2 | 0.1 | 0.3 | 100% charge |
| 14 | S | IN | S | O | 0.1 | 0.1 | 0.1 | 100% charge |
| 15 | S | IN | S | O | 0.2 | 0.1 | 0.3 | 100% charge |

TABLE IV
HIGHEST ENERGY ABSORBED BY SVL AND ITS LOCATION

| ID | No Trapped Charge | | | With Trapped Charge | | |
|----|-------------------|----|-------------|---------------------|------|----|
| | JB № | Ph | Energy (kJ) | ID | JB № | Ph |
| 0 | 98 | A | 4.8 | 8 | 98 | C |
| 1 | 98 | A | 2.4 | 9 | 98 | B |
| 2 | 174 | A | 3.6 | 10 | 167 | A |
| 3 | 167 | C | 1.7 | 11 | 174 | A |
| 4 | 98 | A | 5.4 | 12 | 98 | B |
| 5 | 98 | A | 2.2 | 13 | 98 | A |
| 6 | 174 | A | 5.4 | 14 | 167 | B |
| 7 | 167 | C | 2.8 | 15 | 174 | A |

Fig. 8 illustrates SVL voltages and currents for two switching conditions of with and without trapped charges. It

can be seen that the SVL remains in conduction state longer when there are trapped charges on the cable.

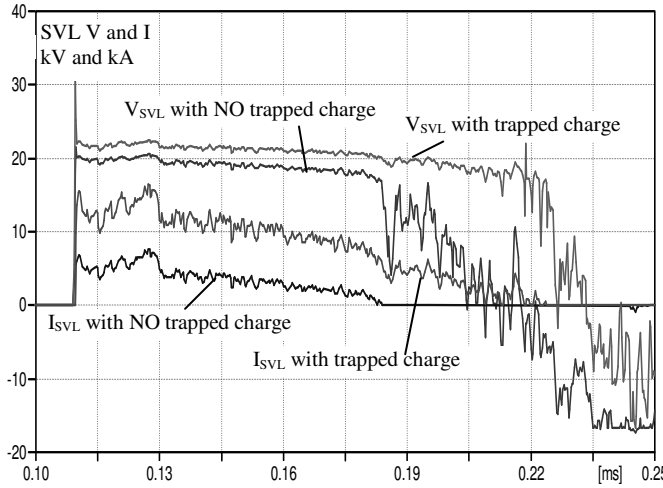


Fig. 8. SVL Voltage and Current at Junction 167 with and Without Trapped Charges, Switch Closed at 0.1 ms.

VII. RECOMMENDATIONS

After study completion, short and long term remedies are proposed. To confirm the existence of trapped charge and its characteristic it is proposed that a survey of trapped charge (standing voltage) on the cable is carried out over several days. High signal bandwidth from measurement equipment is not required. Only transducers insulation and measurement kit are of importance. The result can be used to confirm statistically the level of cable standing voltage and also time constant of the decay, if any, before any significant financial and personnel resources are allocated for remedial work.

As a short term solution with the existing configuration, i.e. no facility to discharge the cable, it is recommended that the cable is first energised from S/S A end, wait at least 30 second or longer and then close the isolator switch L22 in S/S B. It is evident from Table IV that switching from S/S A end would lead to less than rating stress on the SVLs.

As a permanent and viable solution it is suggested that discharge path is provided by changing CVTs at one end of the cable to wound (inductive) instrument transformer type (WVT) with appropriate discharge capability. Not much civil work and rewiring will be involved. WVTs will provide a path to quickly discharge the cable. The path remains available while the cable is out of service and therefore charges and hence voltage on the cable due to proximity remains low. Installing WVTs should be studied at design stage to ensure that low frequency oscillations do not cause any problem.

VIII. CONCLUSIONS

The recommendations in IEC 60071-4, CIGRE WG 02 and 05 are used to model two cable circuits with excessive SVL failure.

It was shown that if the cable is switched with no trapped charges the SVL ratings would not be exceeded. The trapped charge on the cable would cause higher voltages and prolong SVL conduction which causes energy rating of SVLs to exceed. Examination of the substation layouts confirmed that discharge path did not exist for the charges to drain to earth if

the cable is isolated by operating isolation switches L21 and L22. Short and long term solutions are proposed to reduce and then in long term eliminate excessive SVL failures.

IX. APPENDICES

A. Appendix A

The cable is of 275 kV, 1600 mm², copper conductor, oil-filled and paper insulated. The cable layout and spacing is shown in Fig. A. 1. The cable data is given in Table A. 1. The relative permittivity of the insulation around sheath is considered to reduce from 8 at 50 Hz to 4.5 at 5 kHz. The overall cable radius is 5.156 cm. The earth resistivity is considered to be 20 Ω.m throughout.

The cable joint assembly are connected to the crossbonding or solid earth link boxes by concentric bonding leads. These are about 7.5 cm apart with length of 10 m for all link boxes. The concentric cable data is given in

Table A. 2. The overall radius is 2.46 cm.

TABLE A. 1- CABLE DATA

| | Inner Radius (cm) | Outer Radius (cm) | ρ (Ω.m) | μ_{core} | $\mu_{insulation}$ | ϵ_r |
|--------|-------------------|-------------------|------------------------|--------------|--------------------|--------------|
| Core | 0.68 | 2.675 | 1.724×10^{-8} | 1 | 1 | 3.8 |
| Sheath | 4.3 | 4.72 | 2.13×10^{-7} | 1 | 1 | 8 |

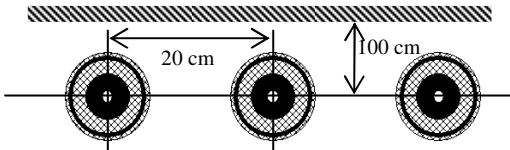


Fig. A. 1. Cable Layout, Spacing and Trench Depth.

TABLE A. 2- CONCENTRIC CABLE DATA

| | Inner Radius (cm) | Outer Radius (cm) | ρ (Ω.m) | μ_{core} | $\mu_{insulation}$ | ϵ_r |
|--------|-------------------|-------------------|------------------------|--------------|--------------------|--------------|
| Core | 0 | 1.25 | 1.724×10^{-8} | 1 | 1 | 3.5 |
| Sheath | 1.75 | 2.16 | 2.826×10^{-8} | 1 | 1 | 1 |

B. Appendix B

Details of overhead lines, used in the simulation are given in TABLE B. 1 and TABLE B. 2. Tower structure is shown in

Fig. B. 1. The lines lengths are given in Table B. 3. The parameters of other cables in the model are given in TABLE B. 4. The data for transformers in the model is given in TABLE B. 5. Note that the magnetising current data is not given for lack of space and also because the magnetising branch current does not greatly affect the conclusion of the study. The positive and zero phase sequence (pps and zps) of self and mutual impedances between nodes of the boundary points are given in TABLE B. 6 and TABLE B. 7 respectively. The pps node capacitances are given in TABLE B. 8. The zps capacitances are the same except for Node B4 which is 10.7 μF. Quad booster impedance is 0.015+j5.15 Ω/ph.

TABLE B. 1- CONDUCTOR DETAILS FOR TRANSMISSION LINE L2/1 AND L2/2

| | Conductor | | Earth Wire | | No Bundle | Bundle d (cm) |
|------|----------------------------|-------------|----------------------------|-----------|--------------|------------------|
| | R _{Outer} (cm) | R (Ω/km) | R _{Outer} (cm) | R Ω/km | | |
| L2/1 | 1.5165 | 0.0589 | 0.9765 | 0.1489 | 2 | 40 |
| L2/2 | 1.431 | 0.0673 | 0.9765 | 0.1489 | 2 | 30 |

TABLE B. 2- TOWER DIMENSION DETAIL FOR TOWER L2/1 AND L2/2

| | X ₁₁ (m) | X ₁₂ (m) | X ₁₃ (m) | X ₂₁ (m) | X ₂₂ (m) | X ₂₃ (m) | X ₀ (m) |
|------|---------------------|---------------------|---------------------|---------------------|---------------------|---------------------|--------------------|
| L2/1 | -5.48 | -5.71 | -6.09 | 5.48 | 5.71 | 6.09 | 0 |
| L2/2 | -5.94 | -8.53 | -6.7 | 5.94 | 8.53 | 6.7 | 0 |

| | Y ₁ (m) | Y ₂ (m) | Y ₃ (m) | Y ₄ (m) |
|------|--------------------|--------------------|--------------------|--------------------|
| L2/1 | 27.24 | 19.47 | 11.63 | 34.14 |
| L2/2 | 30.01 | 20.57 | 12.57 | 39.77 |

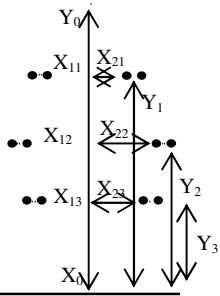


Fig. B. 1. Tower Structure.

TABLE B. 3-LINE LENGTH

| ID | Type | Length (km) |
|----|------|-------------|
| L1 | L2/2 | 5.14 |
| L2 | L2/2 | 8.15 |
| L3 | L2/1 | 38.04 |
| L4 | L2/2 | 26.72 |
| L5 | L2/2 | 8.5 |

TABLE B. 4- NETWORK CABLES PARAMETERS

| ID | R ⁺ mΩ/km | X ⁺ mΩ/km | R ⁰ mΩ/km | X ⁰ mΩ/km | B ⁺ nF/km | B ⁰ nF/km | L km |
|-----|-------------------------|-------------------------|-------------------------|-------------------------|-------------------------|-------------------------|---------|
| C10 | 15.1 | 173.2 | 235.2 | 80.16 | 426.4 | 426.4 | 2.66 |
| C11 | 15.1 | 173.2 | 235.2 | 80.16 | 426.4 | 426.4 | 2.66 |
| C20 | 14.4 | 131.2 | 224.0 | 83.2 | 388.1 | 358.1 | 11.68 |
| C30 | 15.1 | 173.2 | 235.2 | 80.16 | 426.4 | 426.4 | 3.28 |
| C40 | 13.6 | 166.38 | 242.0 | 83.2 | 457.5 | 457.5 | 7.74 |
| C50 | 13.6 | 168.6 | 65.0 | 50.67 | 450.3 | 450.3 | 11.68 |
| C51 | 18.9 | 180.75 | 82.4 | 58.23 | 371.7 | 371.7 | 0.48 |
| C60 | 13.6 | 168.6 | 65.0 | 50.67 | 450.3 | 450.3 | 0.21 |
| C61 | 13.6 | 168.6 | 65.0 | 50.67 | 450.3 | 450.3 | 0.48 |
| C70 | 15.1 | 173.2 | 235.2 | 80.16 | 426.4 | 426.4 | 20.67 |
| C80 | 15.1 | 173.2 | 235.2 | 80.16 | 426.4 | 426.4 | 13.48 |
| C81 | 15.1 | 173.2 | 235.2 | 80.16 | 426.4 | 426.4 | 13.48 |

TABLE B. 5- NETWORK TRANSFORMER DATA

| ID | kV | MVA | HV-MV | | MV-LV | | LV-HV | |
|----|------------|------------|----------|-----------------------|----------|-----------------------|----------|-----------------------|
| | | | X (%) | P _C (W) | X (%) | P _C (W) | X (%) | P _C (W) |
| T1 | 400/275/13 | 950/950/60 | 25.2 | 1265 | 6.6 | 103 | 9.1 | 99.7 |
| T2 | 400/275/13 | 950/950/60 | 25.2 | 1265 | 6.6 | 103 | 9.1 | 99.7 |
| T3 | 400/275/13 | 750/750/60 | 20.1 | 1451 | 8.4 | 114 | 11 | 113 |
| T4 | 400/275/13 | 750/750/60 | 20.1 | 1451 | 8.4 | 114 | 11 | 113 |
| T5 | 400/275/13 | 750/750/60 | 20.1 | 1451 | 8.4 | 114 | 11 | 113 |

TABLE B. 6- SOURCE POSITIVE PHASE SEQUENCE IMPEDANCES

| | B1-1 (Ω) | B1-2 (Ω) | B2 (Ω) | B3-1(Ω) | B3-2 (Ω) | B4 (Ω) |
|------|-----------------|-----------------|----------------|-----------------|----------------|----------------|
| B1-1 | 0.92+ j12.72 | 5.03+ j100.5 | | | | |
| B1-2 | 5.03+ j100.5 | 0.87+ j12.35 | | | | |
| B2 | | | 0.61+ j7.23 | | | |
| B3-1 | | | | 3.09+ j20.42 | 18+ j270.2 | 2.5+ j49.95 |
| B3-2 | | | | | 18+ j20.42 | 2.5+ j49.95 |
| B4 | | | | | 2.5+ j49.95 | 0.84+ j8.69 |

TABLE B. 7- SOURCE ZERO PHASE SEQUENCE IMPEDANCES

| | B1-1 (Ω) | B1-2 (Ω) | B2 (Ω) | B3-1(Ω) | B3-2 (Ω) | B4 (Ω) |
|------|----------------|----------------|----------------|-----------------|-----------------|-----------------|
| B1-1 | 0.58+ j7.29 | 8.4+ j125.7 | | | | |
| B1-2 | 8.4+ j125.7 | 0.73+ j7.45 | | | | |
| B2 | | | 0.83+ j6.79 | | | |
| B3-1 | | | | 3.18+ j25.13 | 1.68+ j25.12 | 7.5+ j157.08 |
| B3-2 | | | | | 1.68+ j25.13 | 1.79+ j14.14 |
| B4 | | | | | 7.5+ j157.08 | 0.1+ j157.08 |

TABLE B. 8- SOURCE POSITIVE PHASE SEQUENCE CAPACITANCES

| | B1-1(μF) | B1-2(μF) | B2(μF) | B3-1(μF) | B3-2(μF) | B4 (μF) |
|------|----------|----------|--------|----------|----------|---------|
| B1-1 | 1.0 | 0.1 | | | | |
| B1-2 | 0.1 | 1.0 | | | | |
| B2 | | | 10.7 | | | |
| B3-1 | | | | 1.0 | 0.1 | 0.1 |
| B3-2 | | | | | 0.1 | 0.5 |
| B4 | | | | | 0.1 | 0.1 |

X. REFERENCES

- [1] W. F. J. Kersten, "Surge arresters for sheath protection in crossbonded cable system," Proc. IEE, Vol. 126, No. 12, Dec 1979, pp 1255-1262.
- [2] N. Nagaoka, A. Ametani, "Transient calculations on crossbonded cables," IEEE Tran. on PAS, Vol. PAS-102, No. 4, April 1983, pp 779-787.
- [3] Y. H. Song, K. Xie, C. Ferguson, "Development of an ATP-based fault simulator for underground power cable," IEEE Power Engineering Society Winter Meeting 2000, Vol. 1, pp 757-761.
- [4] Z. Emin, P. K. Basak, C. Ferguson, "Simulation studies to improve design for midlife 275-kV cable refurbishment," IEEE Trans. on PWRD, Vol. 18, No. 3, July 2003, pp 679-683.
- [5] IEC 60071-4:2004, Insulation Co-ordination, Part 4: Computational guide to insulation co-ordination and modelling of electrical networks.
- [6] CIGRE WG 02, Guidelines for representation of network elements when calculating transients, Working Group 02 of Study Committee 33, Publication 39, 1991-10.
- [7] CIGRE WG 05, The calculation of switching surges, CIGRE Working Group 05, Study Committee No 13, Electra No 62.